Available online at www.sciencedirect.com
SCIENCE DIRECT®
Carbohydrate Research 338 (2003) 1197–1208
CARBOHYDRATE RESEARCH
www.elsevier.com/locate/carres

Structure of the xyloglucan produced by suspension-cultured tomato cells

Zhonghua Jia, Qiang Qin, Alan G. Darvill, William S. York*

Complex Carbohydrate Research Center and Department of Biochemistry and Molecular Biology, University of Georgia, 220 Riverbend Road, Athens, GA 30602-4712, USA

Received 27 November 2002; accepted 12 February 2003

Abstract

The xyloglucan secreted by suspension-cultured tomato (*Lycopersicon esculentum*) cells was structurally characterized by analysis of the oligosaccharides generated by treating the polysaccharide with a xyloglucan-specific endoglucanase (XEG). These oligosaccharide subunits were chemically reduced to form the corresponding oligoglycosyl alditols, which were isolated by high-performance liquid chromatography (HPLC). Thirteen of the oligoglycosyl alditols were structurally characterized by a combination of matrix-assisted laser-desorption ionization mass spectrometry and two-dimensional nuclear magnetic resonance (NMR) spectroscopy. Nine of the oligoglycosyl alditols (GXGGol, XXGGol, GSGGol, XSGGol, LXGGol, XTGGol, LSGGol, LLGGol, and LTGGol, [see, Fry, S.C.; York, W.S., et al., *Physiologia Plantarum* **1993**, *89*, 1–3, for this nomenclature]) are derived from oligosaccharide subunits that have a cellotetraose backbone. Very small amounts of oligoglycosyl alditols (XGGol, XGGXXGGol, XXGGXGGol, and XGGXSGGol) derived from oligosaccharide subunits that have a cellotriose or celloheptaose backbone were also purified and characterized. The results demonstrate that the xyloglucan secreted by suspension-cultured tomato cells is very complex and is composed predominantly of 'XXGG-type' subunits with a cellotetraose backbone. The rigorous characterization of the oligoglycosyl alditols and assignment of their ^{1}H and ^{13}C NMR spectra constitute a robust data set that can be used as the basis for rapid and accurate structural profiling of xyloglucans produced by Solanaceous plant species and the characterization of enzymes involved in the synthesis, modification, and breakdown of these polysaccharides. © 2003 Elsevier Science Ltd. All rights reserved.

Keywords: Xyloglucan; Solanaceae; Cell wall; Structures; *Lycopersicon esculentum*; Nuclear magnetic resonance spectroscopy (NMR)

1. Introduction

Xyloglucan is a hemicellulosic polysaccharide found in the primary (growing) cell walls of all higher plants. In most current models of the primary cell wall,[1–5] xyloglucan and cellulose interact to form a key load-bearing network that prevents the cell from rupturing under osmotic stress. Many of the general structural features of xyloglucans are conserved in all plants. For example, all xyloglucans have a cellulosic (i.e., poly-(1→4)-β-D-Glc*p*) backbone, to which α-D-Xyl*p* residues are linked. Plants as diverse as pine trees (gymnosperms), *Arabidopsis thaliana* (a dicotyledonous angiosperm), and onion (a monotyledonous angiosperm), all produce very similar xyloglucans, in which many of the side chains are terminated with fucosyl residues.

It has been suggested that the conserved fucose-containing side chains facilitate assembly of the xyloglucan–cellulose network[6] and are required for the signaling activity that has been proposed for certain xyloglucan oligosaccharides.[7] However, several mutant plant lines appear to grow normally under greenhouse conditions, despite the fact that they are deficient in the glycosyl transferase (AtFUT1) that catalyzes the transfer of fucose to xyloglucan.[8,9] Furthermore, several plant species, notably members of the *Poaceae* and *Solanaceae*, produce xyloglucans that are devoid of fucose.[3] Clearly, additional information regarding the structural features of xyloglucans from diverse sources is required to understand the fundamental relationships between the biological functions of xyloglucan and

* Corresponding author. Tel.: +1-706-5424401; fax: +1-706-5424412
E-mail address: will@ccrc.uga.edu (W.S. York).

0008-6215/03/$ - see front matter © 2003 Elsevier Science Ltd. All rights reserved.
doi:10.1016/S0008-6215(03)00079-X

their structures. This manuscript describes the detailed structural features of the xyloglucan produced by suspension-cultured cells of the tomato (*Lycopersicon esculentum*), a commercially important, Solanaceous plant.

Most primary cell walls contain xyloglucans that consist of subunit oligoglycosides built around a common heptaglycosyl core, which is composed of a cellotetraose backbone (β-D-Glc*p*-(1→4)-β-D-Glc*p*-(1→4)-β-D-Glc*p*-(1→4)-β-D-Glc*p*), with three of the four β-D-Glc*p* residues bearing an α-D-Xyl*p* residue at O-6. According to a widely used nomenclature for xyloglucans,[10] a β-D-Glc*p* backbone residue with a single α-D-Xyl*p* residue at O-6 is specified by the uppercase letter X and an unbranched β-D-Glc*p* residue is specified by the uppercase letter G. Thus, the heptaglycosyl core described above is designated XXXG, and xyloglucans composed of subunits with this core structure are designated 'XXXG-type' xyloglucans.[11] The cell walls of some plant species, notably the *Solanaceae*, contain 'XXGG-type' xyloglucans, in which only two of the four β-D-Glc*p* residues in the core structure bear α-D-Xyl*p* residues.[12]

The seeds of many plant species contain XXXG-type xyloglucans in which some of the α-D-Xyl*p* residues bear a β-D-Gal*p* residue at O-2, forming diglycosyl side chains. A β-D-Glc*p* residue bearing this side chain is designated by an uppercase L. Accordingly, most seed xyloglucans are composed predominantly of oligoglycosyl subunits designated XLLG, XLXG, XXLG, and XXXG. The primary cell walls of most higher plant species contain XXXG-type xyloglucans that are more complex than the seed xyloglucans. Typically, an α-L-Fuc*p*-(1→2)-β-D-Gal*p* moiety is attached to O-2 of some of the α-D-Xyl*p* residues, forming a triglycosyl side chain. A β-D-Glc*p* residue bearing this triglycosyl side chain is designated by an uppercase F, and most cell wall xyloglucans are composed predominantly of XXXG, XLFG, and XXFG subunits.

Several species in the plant families *Lamiaceae* and *Solanaceae* (both in the subclass *Asteridae*) produce xyloglucans that lack fucose. For example, the fruit of the olive plant (*Olea europaea*, in the *Lamiaceae* family) contains an XXXG-type xyloglucan composed predominantly of XXSG and XLSG subunits,[13] where the uppercase S indicates a β-D-Glc*p* residue bearing an α-L-Ara*f*-(1→2)-α-D-Xyl*p* side chain at O-6. The primary cell walls of several species in the family *Solanaceae* contain XXGG-type xyloglucans. For example, suspension-cultured tobacco cells secrete xyloglucan that lacks fucose and is composed primarily of XSGG and XXGG subunits.[12,14] The xyloglucan secreted by suspension-cultured tomato cells is similar but more complex than tobacco xyloglucan,[12] as it also contains unusual β-L-Ara*f*-(1→3)-α-L-Ara*f*-(1→2)-α-D-Xyl*p* and β-D-Gal*p*-(1→2)-α-D-Xyl*p* side chains, designated T and L, respectively.

A xyloglucan molecule that contains relatively few side chains can still have a complex structure because the side chains can be combined in many different ways to produce oligosaccharide subunits. Nevertheless, the overall structure of the xyloglucan can be determined by purification and analysis of the subunits after their release by treatment of the polysaccharide with a β-(1→4)-endoglucanase. Typically, the endoglucanase selectively cleaves the glycosidic bonds of unbranched β-D-Glc*p* residues of the xyloglucan.[15,16] Thus, almost all of the oligosaccharides generated by endoglucanase-treatment of an XXXG-type xyloglucan contain a cellotetraose backbone. In contrast, each subunit of an XXGG-type xyloglucan contains two potential endoglucanase-susceptible sites,[16] so endoglucanase treatment of an XXGG-type xyloglucan can generate oligosaccharides with from three to five β-D-Glc*p* residues in the backbone.[12] However, one of the two potentially susceptible β-D-Glc*p* residues in the xyloglucans produced by Solanaceous plants usually bears an *O*-acetyl substituent at O-6, rendering it resistant to endoglucanase-catalyzed hydrolysis.[12,14] Thus, endoglucanase treatment of endogenously *O*-acetylated tomato xyloglucan generates a set of well-defined, XXGG-type oligosaccharide subunits, which are described in this manuscript.

2. Results

2.1. Isolation of xyloglucan oligoglycosyl alditols

A mixture of polysaccharides, including xyloglucan, galactoglucomannan and pectin, was prepared by ethanol precipitation from the spent medium of suspension-cultured tomato cells. After removing pectic polysaccharides by anion-exchange chromatography, the mixture of polysaccharides was treated with a xyloglucan-specific endoglucanase (XEG),[15] which specifically hydrolyzes unbranched β-D-Glc*p* residues of the xyloglucan, leaving the galactoglucomannan unaltered. The resulting xyloglucan oligosaccharides were separated from the galactoglucomannan by ethanol precipitation. In order to facilitate their separation and characterization, the oligosaccharides were reduced with sodium borohydride, converting them to oligoglycosyl alditol derivatives. The oligoglycosyl alditol mixture was analyzed by matrix-assisted laser-induced/ionization time-of-flight mass spectrometry (MALDI-TOF MS), indicating the presence of at least eight major components and at least three minor components (Table 1).

Oligoglycosyl alditols were separated into size classes by size-exclusion chromatography on Bio-Gel P-2. Individual fractions for the P-2 column were then injected onto a reversed-phase high-performance liquid chro-

matography (HPLC) column and eluted with a methanol–water gradient. HPLC fractions were analyzed by MALDITOF MS, and those that contained a single oligoglycosyl alditol by this criterion were fully characterized by NMR spectroscopy and other methods, when appropriate.

2.2. NMR analysis of oligoglycosyl alditols

Purified oligoglycosyl alditols were characterized in D_2O by one- and two-dimensional NMR spectroscopy (Tables 2–4). Each glycosyl residue of an oligoglycosyl alditol comprises a magnetically isolated set of nuclei, as homonuclear scalar coupling between nuclei that are not in the same residue is very small (but not necessarily zero, see below). The scalar coupling connectivity between the nuclei can be traced within each residue by gCOSY, TOCSY, and HSQC experiments, making it possible to assign each ^1H and ^{13}C NMR resonance to a distinct residue.

Linkages between glycosyl residues were assigned by several complementary approaches. The initial assignment of glycosyl linkages were based on NOE contacts between H-1 resonances and resonances of the aglyconic residues. For example, NOE contacts between H-1 of an α-D-Xyl*p* residue and both H-6 resonances of the β-D-Glc*p* residue to which it is linked are diagnostic for the α-(1→6) linkage connecting an α-D-Xyl*p* residue to a specific β-D-Glc*p* residue in the xyloglucan backbone. However, NOE contacts are not always diagnostic for the site of attachment for a glycosidic linkage, as the NOE depends on the distance between nuclei rather than the molecular bond network connecting them.[17] For example, in addition to the strong interglycosidic H-1–H-4′ NOE contact that is expected for adjacent β-D-Glc*p* residues in the β-(1→4)-linked xyloglucan backbone, we routinely observe relatively weak interglycosidic H-1–H-6′R and H-1–H-6′S NOEs. Although the latter NOEs are useful in assigning the *sequence* of β-D-Glc*p* residues in the xyloglucan backbone, it would be incorrect to interpret them as indicating the presence of a β-(1→6) linkage. In rare cases, an NOE contact can even exist between glycosyl residues that are not directly linked to each other. For example, in the NOESY spectrum of LTGGol, α-Ara[b] H-5 has a weak NOE contact with Glc[a] H-1, which is 18 bonds away. (See Fig. 1, peak 1G[a]-5α[b], and Fig. 2 for nomenclature describing each oligoglycosyl alditol and the nuclei within.)

Table 1
MALDITOF MS of xyloglucan oligoglycosyl alditols from cultured tomato cells

m/z [a]	Deduced composition	Abundance [b]	Structure(s)
662	$Hexose_3Pentose$	trace	XGGol
824	$Hexose_4Pentose$	3	GXGGol
956	$Hexose_4Pentose_2$	11	XXGGol (70%) GSGGol (30%)
1088	$Hexose_4Pentose_3$	20	XSGGol
1118	$Hexose_5Pentose_2$	14	LXGGol
1220	$Hexose_4Pentose_4$	10	XTGGol
1250	$Hexose_5Pentose_3$	22	LSGGol
1280	$Hexose_6Pentose_2$	13	LLGGol
1382	$Hexose_5Pentose_4$	7	LTGGol
1574	$Hexose_7Pentose_3$	trace	XGGXXGGol XXGGXGGol
1706	$Hexose_7Pentose_4$	trace	XGGXSGGol

[a] Chemical mass of the $[M+Na]^+$ ion.
[b] Normalized percent.

Table 2
Assignment of the HMBC spectrum of LTGGol

^1H Assignment	δ ^1H	^{13}C Assignment	δ ^{13}C	Comment
α-Ara[b] H-1	5.181	α-Ara[b] C-3	85.9	weak
α-Ara[b] H-1	5.181	α-Ara[b] C-4	85.0	
α-Ara[b] H-1	5.181	Xyl[b] C-2	81.9	1,2 link
Xyl[c] H-1	5.155	Xyl[c] C-2	83.0	
Xyl[c] H-1	5.155	Xyl[c] C-3	74.6	weak
Xyl[c] H-1	5.155	Glc[c] C-6	69.4	1,6 link
Xyl[c] H-1	5.155	Xyl[c] C-5	63.7	
β-Ara[b] H-1	5.096	α-Ara[b] C-3	85.9	1,3 link
β-Ara[b] H-1	5.096	β-Ara[b] C-4	84.7	
β-Ara[b] H-1	5.096	β-Ara[b] C-2	79.1	weak
β-Ara[b] H-1	5.096	β-Ara[b] C-3	76.9	
Xyl[b] H-1	5.088	Xyl[b] C-2	81.9	weak
Xyl[b] H-1	5.088	Xyl[b] C-3	74.5	
Xyl[b] H-1	5.088	Glc[b] C-6	69.7	1,6 link
Xyl[b] H-1	5.088	Xyl[b] C-5	63.7	
Glc[a] H-1	4.596	Glcol C-4	81.8	1,4 link
Glc[b] H-1	4.573	Glc[a] C-4	81.7	1,4 link
Gal[c] H-1	4.561	Xyl[c] C-2	83.0	1,2 link
Glc[c] H-1	4.505	Glc[b] C-4	82.6	1,4 link
α-Ara[b] H-3	3.961	β-Ara[b] C-1	104.0	1,3 link
β-Ara[b] H-4	3.911	β-Ara[b] C-1	104.0	
Glc[c] H-6	3.879	Xyl[c] C-1	100.9	1,6 link
Xyl[c] H-5	3.718	Xyl[c] C-1	100.9	
Xyl[b] H-5	3.723	Xyl[b] C-1	101.3	
Glcol H-4	3.868	Glc[a] C-1	105.0	1,4 link
Glc[a] H-2	3.392	Glc[a] C-1	105.0	
Glc[a] H-4	3.727	Glc[b] C-1	105.1	1,4 link
Glc[b] H-2	3.399	Glc[b] C-1	105.1	
Glc[b] H-4	3.643	Glc[c] C-1	105.6	1,4 link
Glc[c] H-2	3.329	Glc[c] C-1	105.6	
Xyl[c] H-2	3.683	Gal[c] C-1	107.1	1,2 link
Gal[c] H-2	3.606	Gal[c] C-1	107.1	
Xyl[b] H-2	3.567	α-Ara[b] C-1	112.2	1,2 link

Only those long-range heteronuclear correlations involving anomeric protons or carbons are listed. [a,b,c]Indicates the position of the residue in the oligoglycosyl alditol (see Fig. 2).

Strong scalar coupling between two nuclei in the same residue can lead to NOESY crosspeaks for pairs of nuclei that are not close together in space.[18] For example, the relatively weak crosspeak correlating H-1 of Glc^c with H-3 of Glc^b in the NOESY spectrum of LTGGol (Fig. 1, dashed box) may be due to a combination of the direct interaction of H-1 of Glc^c with H-4 of Glc^b and strong scalar coupling between H-3 and H-4 of Glc^b. Similar, presumably indirect interactions lead to crosspeaks correlating H-1 of Glc^c with H-5 of Glc^b, and H-1 of Xyl^b with H-5 of Glc^b. Alternatively, indirect NOE crosspeaks can be due to the 'three-spin effect', in which an NOE observed between two nuclei is mediated by a third nucleus that is close in space to both.[18] For the oligoglycosides described here, $\omega\tau_c$ is greater than 1.12 (i.e., within the negative NOE regime), making it difficult to distinguish three-spin effects from direct NOEs. Furthermore, one cannot rule out the possibility that some of the crosspeaks listed above are not due to indirect interactions, but represent true NOE contacts between nuclei that transiently come into close proximity due to internal motion of the molecule.

As the glycosyl linkages cannot be unambiguously assigned from the NOESY data, they were confirmed by detecting long-range, interglycosidic, scalar coupling. For example, $^3J_{C1Hx}$ and $^3J_{H1Cx}$ couplings were detected by HMBC experiments when sufficient material was available. Long-range homonuclear scalar couplings ($^4J_{HH}$) were also detected by recording two-dimensional gCOSY spectra at high-resolution and high-signal-to-noise.[19] The gCOSY spectrum of LTGGol is shown in Fig. 1 as an example. Typically, gCOSY crosspeaks due to long-range couplings ($^4J_{HH}$ and $^5J_{HH}$) were less than 10% as intense as crosspeaks due to vicinal coupling ($^3J_{HH}$). Interglycosidic $^4J_{H1Hx}$ coupling was observed for six of the eight glycosidic linkages in LTGGol, and only the α-D-Xyl*p*-(1→6)-β-D-Glc*p* linkages were devoid of observable long-range, homonuclear coupling. The $^4J_{H1H3'}$ coupling corresponding to the (1→3) linkage between the β-Ara*f* and the α-Ara*f* residues and the $^4J_{H1H2'}$ coupling corresponding to the (1→2) linkages between the α-Ara*f* and α-Xyl*p* residues were visible, but very weak. Therefore, it was necessary to use long-range *heteronuclear* coupling (observed in the HMBC spectrum, Table 2) to confirm the sequence and linkages of the Ara-Ara-Xyl side chain and the attachment sites of each α-D-Xyl*p* residue to the backbone of LTGGol.

Many of the assignments of resonances to nuclei within specific glycosyl residues (initially made on the basis of the vicinal couplings) were confirmed by observation of long-range *intraglycosidic* couplings observed in the gCOSY spectra. As previously observed,[19] intraglycosidic long-range coupling was observed only rarely within β-pyranosyl residues (β-D-Glc*p* and β-D-Gal*p*). For example, the only long-range coupling detected within the β-pyranosyl residues of LTGGol was $^4J_{H1H3}$ in the β-D-Gal*p* residue (Fig. 1, peak 1L^c-3L^c). Intraglycosidic long-range coupling was much more apparent within α-D-Xyl*p* residues, as relatively strong crosspeaks corresponding to $^4J_{H1H3}$ and $^4J_{H1H5a}$ within Xyl*p* residues were frequently observed. The α- and β-Ara*f* residues exhibited distinct intraglycosidic long-range coupling patterns. In α-Ara*f* residues, $^4J_{H1H3}$ was relatively strong, while $^5J_{H1H5R}$, $^5J_{H1H5S}$, and $^4J_{H1H4}$ were extremely weak. In β-Ara*f* residues, $^4J_{H1H3}$, $^5J_{H1H5R}$, and $^5J_{H1H5S}$ were all relatively strong, while $^4J_{H1H4}$ was very weak.

2.3. Structural analysis of oligoglycosyl alditols with 10 or more residues

Several larger oligoglycosyl alditols, which contained XEG-susceptible β-D-Glc*p* residues, were isolated from the reduced XEG-digest of tomato xyloglucan. These included two isomers ($[M+Na]^+$ m/z 1574, reduced Hex_7Pent_3) that lack Ara*f* residues, and an oligoglycosyl alditol ($[M+Na]^+$ m/z 1706, reduced Hex_7Pent_4) with one Ara*f* residue. The MS data suggest that each of these oligoglycosyl alditols are derived from oligosaccharides that have a heptaglucosyl backbone, i.e., each is composed of an XXGG- and XGG-type subunits, which remained attached during the XEG-digestion. Although NMR analysis of these large oligoglycosyl alditols is difficult due to signal overlap, sufficient information could be extracted from the NMR spectra to deduce their basic structures as follows. Each of these oligoglycosyl alditols yields a ^{1}H NMR spectrum with six anomeric proton resonances assigned to β-D-Glc*p* residues and three anomeric protons assigned to α-D-Xyl*p* residues (Table 3), along with alditol resonances, which were not assigned. (The spectrum of the m/z 1706 oligoglycosyl alditol has one additional anomeric proton resonance, assigned to an α-L-Ara*f* residue.) The β-D-Glc*p* residue at the nonreducing end of the backbone of each oligoglycosyl alditol bears an α-D-Xyl*p* residue at O-6, as indicated by a resonance whose chemical shift and coupling pattern (δ 4.940, $^3J_{H1H2}$ 3.6 Hz) is characteristic of the anomeric proton of an α-D-Xyl*p* residue in this environment (Table 3).[12,13,20–24] Interglycosidic NOE contacts between this α-D-Xyl*p* anomeric resonance and H-6R–H-6S of the β-D-Glc*p* to which it is attached allow resonances of the β-D-Glc*p* residue at the nonreducing end of each main chain to be assigned. Interglycosidic H-1–H-4′ and H-1–H-6′ NOEs then allow the resonances of the penultimate β-D-Glc*p* residue in each sequence to be identified. The substitution pattern of the penultimate β-D-Glc*p* residue of each of the large oligoglycosyl alditols was deduced from the chemical shifts (Table 3) of diagnostic resonances and other

Table 3
^{1}H NMR assignments for the oligoglycosyl alditols

Sugar	H-1′	H-1	H-2	H-3	H-4	H-5$_a$	H-5$_e$	H-6	H-6′
XGGol									
Xyl[b]		4.940	3.544	3.727	3.611	3.551	3.708		
Glc[b]		4.549	3.329	3.52	3.52	3.700		3.778	3.937
Glc[a]		4.596	3.380	3.656	3.681	3.581		3.859	3.963
Glcol	3.641	3.781	3.958	3.838	3.867	3.938		3.742	3.868
GXGGol									
Xyl[b]		4.959	3.543	3.722	3.618	3.571	3.733		
Glc[c]		4.519	3.322	3.507	3.413	3.481		3.733	3.917
Glc[b]		4.562	3.382	3.666	3.738	3.819		3.900	4.007
Glc[a]		4.595	3.383	3.647	3.69	3.585		3.856	3.960
Glcol	3.640	3.783	3.956	3.838	3.868	3.940		3.814	3.743
GSGGol[d]									
α-Ara[b]		5.169	4.201	3.935	4.082	3.848	3.710		
Xyl[b]		5.096	3.573	3.856	3.661	3.564	3.733		
Glc[c]		4.511	3.315	3.507	3.415	3.474		3.736	3.918
Glc[b]		4.548	3.389	3.661	3.691	3.837		3.952	3.952
Glc[a]		4.597	3.389	3.645	3.689	3.587		3.857	3.976
Glcol	3.641	3.781	3.957	3.838	3.868	3.938		3.742	3.866
XXGGol[d]									
Xyl[c]		4.940	3.544	3.733	3.612	3.551	3.715		
Xyl[b]		4.956	3.544	3.725	3.612	3.574	3.725		
Glc[c]		4.553	3.341	3.52	3.52	3.698		3.782	3.935
Glc[b]		4.566	3.393	3.674	3.733	3.829		3.904	4.007
Glc[a]		4.597	3.385	3.649	3.687	3.584		3.854	3.957
Glcol	3.640	3.780	3.955	3.839	3.867	3.941		3.742	3.873
XSGGol[d]									
α-Ara[b]		5.169	4.199	3.934	4.084	3.848	3.712		
Xyl[c]		4.939	3.554	3.732	3.615	3.544	3.713		
Xyl[b]		5.094	3.572	3.857	3.662	3.583	3.588		
Glc[c]		4.543	3.331	3.52	3.52	3.689		3.776	3.942
Glc[b]		4.552	3.396	3.672	3.691	3.845		3.954	3.954
Glc[a]		4.596	3.388	3.646	3.707	3.587		3.857	3.963
Glcol	3.643	3.785	3.966	3.842	3.866	3.941		3.746	3.879
XTGGol									
β-Ara[b]		5.096	4.155	4.093	3.912	3.824	3.745		
α-Ara[b]		5.182	4.411	3.968	4.166	3.851	3.735		
Xyl[c]		4.940	3.543	3.729	3.611	3.558	3.715		
Xyl[b]		5.089	3.569	3.872	3.653	3.581	3.721		
Glc[c]		4.525	3.325	3.518	3.529	3.679		3.772	3.941
Glc[b]		4.564	3.390	3.661	3.651	3.864		3.933	3.933
Glc[a]		4.596	3.390	3.645	3.725	3.586		3.856	3.957
Glcol	3.643	3.783	3.859	3.844	3.864	3.941		3.747	3.875
LXGGol[d]									
Gal[c]		4.562	3.614	3.660	3.924	3.691		3.772	3.772
Xyl[c]		5.160	3.686	3.915	3.667	3.565	3.729		
Xyl[b]		4.956	3.542	3.726	3.615	3.592	3.731		
Glc[c]		4.542	3.346	3.519	3.459	3.739		3.816	3.883
Glc[b]		4.572	3.402	3.684	3.758	3.833		3.902	4.011
Glc[a]		4.595	3.384	3.649	3.691	3.582		3.856	3.957
Glcol	3.645	3.782	3.955	3.837	3.868	3.938		3.875	3.744

Table 3 (*Continued*)

Sugar	H-1′	H-1	H-2	H-3	H-4	H-5$_a$	H-5$_e$	H-6	H-6′
LSGGol									
Gal^c		4.557	3.609	3.652	3.992	3.687		3.763	3.763
α-Ara^b		5.165	4.201	3.932	4.081	3.848	3.709		
Xyl^c		5.156	3.684	3.910	3.661	3.562	3.714		
Xyl^b		5.091	3.569	3.856	3.669	3.566	3.725		
Glc^c		4.527	3.334	3.514	3.452	3.73		3.810	3.883
Glc^b		4.557	3.404	3.682	3.689	3.848		3.951	3.951
Glc^a		4.594	3.387	3.644	3.711	3.584		3.856	3.957
Glcol	3.639	3.781	3.955	3.839	3.863	3.937		3.740	3.873
LLGGol									
Gal^c		4.562	3.614	3.674	3.920	3.688		3.776	3.776
Gal^b		4.559	3.622	3.663	3.920	3.688		3.776	3.776
Xyl^c		5.162	3.686	3.919	3.674	3.567	3.721		
Xyl^a		5.174	3.674	3.913	3.658	3.593	3.730		
Glc^c		4.523	3.348	3.518	3.461	3.742		3.818	3.884
Glc^b		4.576	3.417	3.663	3.680	3.918		3.920	3.979
Glc^a		4.602	3.399	3.664	3.727	3.591		3.863	3.962
Glcol	3.643	3.785	3.960	3.840	3.869	3.941		3.746	3.876
LTGGol									
Gal^c		4.561	3.605	3.658	3.921	3.682		3.76	3.76
β-Ara^b		5.096	4.159	4.091	3.914	3.824	3.746		
α-Ara^b		5.181	4.415	3.963	4.156	3.853	3.735		
Xyl^c		5.156	3.683	3.906	3.659	3.561	3.715		
Xyl^b		5.088	3.568	3.877	3.652	3.578	3.721		
Glc^c		4.506	3.329	3.511	3.452	3.724		3.811	3.881
Glc^b		4.573	3.398	3.681	3.644	3.881		3.911	3.946
Glc^a		4.597	3.393	3.646	3.727	3.586		3.858	3.957
Glcol	3.641	3.781	3.958	3.838	3.867	3.938		3.742	3.866
XGGXXGGol									
Xyl$^{b'}$		4.940	3.541	3.726	3.610	3.550	3.713		
Xyl^c		4.958	3.543	3.724	3.620	3.570	3.724		
Xyl^b		4.958	3.543	3.724	3.620	3.570	3.724		
Glc$^{b'}$		4.537	3.329	3.517	3.517	3.693		3.780	3.935
Glc$^{a'}$		4.529	3.363	3.66	3.66	3.620		3.825	3.980
Glc$^{s'}$		4.543	3.366	3.66	3.66	3.620		3.825	3.980
Glc^c		4.566	3.393	3.674	3.746	3.820		3.894	4.010
Glc^b		4.566	3.393	3.674	3.746	3.820		3.894	4.010
Glc^a		4.594	3.383	3.656	3.683	3.584		3.857	3.959
XXGGXGGol									
Xyl$^{c'}$		4.940	3.542	3.732	3.611	3.551	3.714		
Xyl$^{b'}$		4.958	3.541	3.720	3.618	3.572	3.725		
Xyl^b		4.958	3.541	3.720	3.618	3.572	3.725		
Glc$^{c'}$		4.554	3.337	3.519	3.519	3.679		3.781	3.935
Glc$^{b'}$		4.555	3.387	3.663	3.736	3.814		4.006	3.893
Glc$^{a'}$		4.531	3.365	3.65	3.65	3.623		3.822	3.975
Glc$^{s'}$		4.544	3.365	3.65	3.65	3.623		3.822	3.975
Glc^b		4.561	3.380	3.668	3.743	3.816		4.006	3.893
Glc^a		4.595	3.382	3.656	3.683	3.584		3.857	3.959

Table 3 (*Continued*)

Sugar	H-1′	H-1	H-2	H-3	H-4	H-5_a	H-5_e	H-6	H-6′
XGGXSGGol									
α-Ara[a]		5.165	4.198	3.930	4.087	3.843	3.707		
Xyl[b′]		4.940	3.541	3.726	3.610	3.541	3.710		
Xyl[c]		4.954	3.542	3.720	3.619	3.555	3.724		
Xyl[b]		5.086	3.568	3.847	3.658	3.557	3.725		
Glc[b′]		4.537	3.329	3.517	3.517	3.693		3.780	3.935
Glc[a′]		4.530	3.360	3.66	3.66	3.619		3.825	3.978
Glc[s′]		4.543	3.365	3.66	3.66	3.619		3.825	3.978
Glc[c]		4.556	3.382	3.674	3.743	3.806		3.888	4.010
Glc[b]		4.551	3.395	3.664	3.694	3.827		3.945	3.945
Glc[a]		4.593	3.383	3.656	3.683	3.584		3.857	3.959

[a,b,c]Indicates the position of the residue in the oligoglycosyl alditol (see Fig. 2). [d]Partial assignment of the ^{1}H NMR spectra of the indicated oligoglycosyl alditols was previously reported in Ref. 12.

considerations.[12,13,20–24] For example, the H-4 resonance of a 4-linked β-D-Glc*p* residue is typically about 0.1 ppm upfield of the H-4 resonance of a 4,6-linked β-D-Glc*p* residue that has an α-D-Xyl*p* residue at O-6. Accordingly, the penultimate β-D-Glc*p* residue of one of the arabinose-free (*m*/*z* 1574) oligoglycosyl alditols is (unbranched) 4-linked (i.e., H-4 at δ 3.62) and the penultimate β-D-Glc*p* residue of the other arabinose-free (*m*/*z* 1574) oligoglycosyl alditol is (branched) 4,6-linked (i.e., H-4 at δ 3.74). The penultimate β-D-Glc*p* residue of the arabinose-containing (*m*/*z* 1706) oligoglycosyl alditol is (unbranched) 4-linked (i.e., H-4 at δ 3.65). Analysis of the complete data (Table 3) set strongly indicates that the two (*m*/*z* 1574) isomers are XGGXXGGol and XXGGXGGol, and that the arabinose-containing oligoglycosyl alditol (*m*/*z* 1706) is XGGXSGGol.

The structures XGGXXGGol, XXGGXGGol, and XGGXSGGol each contain at least one XEG-susceptible glycosidic bond, allowing their structures to be confirmed by enzymatic analysis. Borohydride reduction removed any *O*-acetyl substituents that might have been present in the native oligosaccharides, making the oligoglycosyl alditols more susceptible to XEG-catalyzed hydrolysis. Therefore, these oligoglycosyl alditols were digested with XEG, and the products were analyzed by MALDITOF MS. Ideally, unambiguous sequence information could be obtained by this analysis, as fragments derived from the alditol end are characterized by the presence of two more hydrogen atoms than homologous fragments derived from the nonreducing end. Unfortunately, the mass accuracy of the spectrometer used was not sufficient to confidently make this distinction for the (*m*/*z* 1574) oligoglycosyl alditol isomers. However, this distinction is readily made after per-*O*-acetylation of the XEG-generated fragments, as the mass of a per-*O*-acetylated alditol is 44 Da greater than that of the corresponding per-*O*-acetylated reducing sugar. Therefore, XEG-generated fragments of the two (*m*/*z* 1574) oligoglycosyl alditol isomers were per-*O*-acetylated and analyzed by MALDITOF MS. The data obtained by this analysis (Table 5) are consistent with the structural assignments based on NMR analysis. The results indicate that XGGXXGGol and XGGXSGGol were cleaved to form (XGG + XXGGol) and (XGG + XSGGol), respectively, indicating that each has one predominant XEG-susceptible site. In contrast, XXGGXGGol has two XEG susceptible sites, producing two sets of fragments, (XXG + GXGGol) and (XXGG + XGGol).

3. Discussion

The rigorous characterization of the oligoglycosyl alditol derivatives of the oligosaccharide subunits of tomato xyloglucan, along with assignment of their ^{1}H and ^{13}C NMR spectra (Tables 3 and 4), constitute a data set that can be used as the basis for structural profiling of XXGG-type xyloglucans. The data described here reveals many correlations between specific structural features of the oligoglycosyl alditols and the chemical shifts of diagnostic resonances in their NMR spectra. This type of analysis (sometimes called the 'structural–reporter' approach[25]) is facilitated by databases that allow users to retrieve chemical shift data on the basis of structural constraints or vice versa. We maintain an on-line database of this type (http://www.ccrc.uga.edu/xgdb.html) for the analysis of xyloglucan oligoglycosyl alditols at the Complex Carbohydrate Research Center at the University of Georgia. This database already contains a large amount of spectral information for XXXG-type xyloglucans, and many of the structure/chemical shift correlations embodied in the data presented here have been previously described.[12,13,20–24] For example, previous analy-

Table 4
^{13}C NMR assignments for the oligoglycosyl alditols

	C-1	C-2	C-3	C-4	C-5	C-6
GXGGol						
Xyl[b]	101.6[d]	74.2	75.7	72.2	64.3	
Glc[a]	105.0	75.8[e]	76.8	81.4	77.2	62.5
Glc[b]	105.1	75.6[e]	76.8	81.4	76.1	68.8
Glc[c]	105.3	75.8	78.2	72.2	78.8	63.3
Gol	65.3	74.9	72.2	81.8	73.8	64.7
GSGGol						
α-Ara[b]	111.9[d]	83.9	79.1	86.4	63.8	
Xyl[b]	101.3	81.9	74.5	72.1	63.9	
Glc[a]	105.0	75.8	76.8	81.6	77.3	62.5
Glc[b]	105.2	75.5	76.8	81.7	76.5	69.0
Glc[c]	105.4	75.9	78.2	72.2	78.8	63.3
Gol	65.3	74.9	72.2	81.8	73.8	64.7
LXGGol						
Xyl[b]	101.5	74.2	75.7	72.2	64.2	
Xyl[c]	100.9	82.9	74.6	72.1	63.7	
Glc[a]	105.0	75.8	76.8	81.8	77.3	62.4
Glc[b]	105.1	75.5	76.8	82.1	76.0	68.8
Glc[c]	105.5	75.7	78.1	72.6	77.2	69.4
Gal[c]	107.1	73.7	75.3	71.3	77.8	63.6
Gol	65.3	74.9	72.2	81.7	73.8	64.7
XTGGol						
α-Ara[b]	112.3	82.7	86.0	85.0	63.8	
β-Ara[b]	103.9	79.1	76.9	84.7	65.6	
Xyl[b]	101.3	81.9	74.6	72.2	63.8	
Xyl[c]	101.0	78.3	75.8	72.1	63.7	
Glc[a]	105.0	75.8	76.8	81.7	77.2	62.5
Glc[b]	105.1	75.4	76.8	82.5	76.5	69.5
Glc[c]	105.7	75.8	78.3	72.1	77.0	68.6
Gol	65.3	74.9	72.1	81.8	73.7	64.7
LSGGol						
α-Ara[b]	111.9	83.8	79.1	86.5	63.9	
Xyl[b]	101.3	81.5	74.6	72.1	63.7	
Xyl[c]	100.9	83.0	74.6	72.1	63.9	
Glc[a]	105.0	75.8	76.9	81.6	77.2	62.5
Glc[b]	105.1	75.5	76.9	82.4	76.4	69.2
Glc[c]	105.5	75.7	78.2	72.6	77.3	69.5
Gal[c]	107.1	73.7	75.3	71.3	77.8	63.7
Gol	65.3	74.9	72.1	81.8	73.7	64.7
LLGGol						
Xyl[b]	101.4	82.9	74.6	72.1	63.8	
Xyl[c]	100.9	82.9	74.6	72.1	63.7	
Glc[a]	105.0	75.8	77.0	81.5	77.3	62.5
Glc[b]	105.0	75.5	76.9	82.3	76.3	69.5
Glc[c]	105.6	75.7	78.2	72.6	77.2	69.4
Gal[b/c]	107.2	73.7	75.3	71.3	77.8	63.7
Gol	65.3	74.9	72.2	81.7	73.8	64.7
LTGGol						
α-Ara[b]	112.3	82.6	86.0	85.0	63.8	
β-Ara[b]	103.9	79.1	76.9	84.8	65.6	
Xyl[b]	101.3	81.9	74.5	72.1	63.7	
Xyl[c]	100.9	82.9	74.6	72.1	63.7	
Glc[a]	105.0	75.8	76.8	81.8	77.2	62.5
Glc[b]	105.1	75.4	76.8	82.6	76.4	69.6
Glc[c]	105.6	75.8	78.2	72.5	77.1	69.4
Gal[c]	107.1	73.7	75.3	71.3	77.8	63.6
Gol	65.3	74.9	72.1	81.8	73.7	64.7

[a,b,c]Indicates the position of the residue in the oligoglycosyl alditol (see Fig. 2). [d]Chemical shifts measured by the HSQC experiment. [e]Assignments may be reversed.

ses have firmly established that the presence of an 'X' structure at the nonreducing end of the main chain (i.e., the last β-D-Glc*p* residue in the chain bears a terminal α-D-Xyl*p* residue at O-6, as in XXGGol and XSGGol, etc.) is correlated to a doublet ($^3J_{1,2}$ 3.6 Hz) at δ 4.940 (H-1 of the α-D-Xyl*p* residue). This correlation was a critical factor in the structural characterization of the larger oligoglycosyl alditols described here. An important correlation that is now firmly established by the data presented in Table 3 is the side chain-dependent shift of H-4 of 6-substituted β-D-Glc*p* residues at the nonreducing end of the backbone. That is, when the

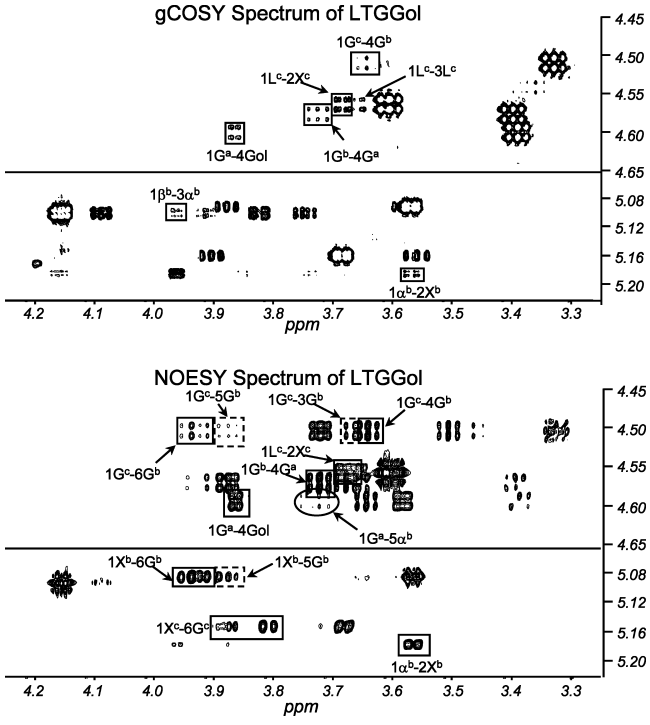

Fig. 1. Two-dimensional NMR spectra of LTGGol, the most complex oligoglycosyl alditol described in this paper. Spectral regions containing crosspeaks between anomeric protons and ring protons are shown. Boxes are drawn around interglycosidic correlations. Each nucleus is identified by three characters: the number indicates the position within the residue; the letter indicates the sugar residue (α ≡ α-Ara*f*, β ≡ β-Ara*f*, G ≡ β-Glc*p*, L ≡ β-Gal*p*, X ≡ α-Xyl*p*); the superscript letter indicates the position of the glucosyl residue or side chain vis a vis the alditol residue of oligoglycoside (see Fig. 2). Thus, 1β^b-3α^b indicates a correlation between H-1 of the β-Ara*f* residue and H-3 of the α-Ara*f* residue, both of which are located in side chain b (i.e., the side chain attached to the central glucosyl residue). (Top Panel) gCOSY spectrum of LTGGol, showing very low-level contours. Intraglycosidic and interglycosidic long-range correlations are visible in addition to the very strong vicinal and geminal correlations normally seen in COSY spectra. (Bottom Panel) NOESY spectrum of LTGGol. An NOE contact between H-1 of Glc^a and H-5 of α-Ara^b (circled 1G^a-5α^b) is observed, even though these two nuclei are 18 bonds apart. Several interglycosidic crosspeaks (dotted boxes) are assigned as indirect interactions (see text).

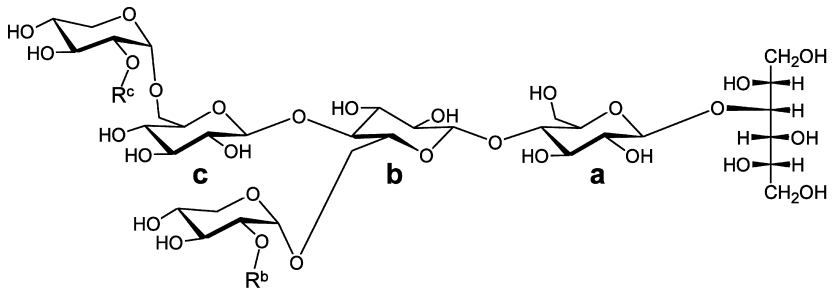

Structure	R^c	R^b
XXGGol	H	H
XSGGol	H	α-L-Ara*f*
LXGGol	β-D-Gal*p*	H
XTGGol	H	β-L-Ara*f*-(1→3)-α-L-Ara*f*
LSGGol	β-D-Gal*p*	α-L-Ara*f*
LLGGol	β-D-Gal*p*	β-D-Gal*p*
LTGGol	β-D-Gal*p*	β-L-Ara*f*-(1→3)-α-L-Ara*f*

Fig. 2. Tomato xyloglucan oligosglycosyl alditols that were characterized. As indicated, these structures are explicitly specified by the commonly used shorthand nomenclature[10] in which each Glc*p* residue in the backbone is indicated by a single uppercase letter (X, L, S, T, G, etc.), which indicates the structure of its attached side chain(s). All of the oligoglycosyl alditols shown are built around a XXGGol core, illustrated at the top. For the purposes of reporting NMR parameters (Tables 2–4), each Glc*p* residue and the side chain attached to it is specified by a lower case, superscript letter (a, b, or c), which indicates the location of the residue vis a vis the alditol residue. That is, Glc^a is the Glc*p* residue linked to the alditol, Glc^b is linked to Glc^a, and Glc^c is linked to Glc^b. In larger oligoglycosyl alditols that contain two subunits (e.g., XGGXXGGol, XXGXGGol, and XGGXSGGol, not shown), residues of the alditol-containing subunit are specified as shown here and residues of the nonreducing end subunit are labeled with superscript c′ (when present), b′, a′ or s′, where the s indicates an XEG-susceptible Glc*p* residues next to a branched Glc*p* residue in the native xyloglucan. (i.e., upon XEG-catalyzed hydrolysis and borohydride reduction, $Glc^{s'}$ would be converted to an alditol.) Residues in each side chain are indicated by the letter designating the Glc*p* residue to which the side chain is attached. For example, the α-Xyl*p* residue linked to Glc^c is called Xyl^c. In this Figure, R^c and R^b indicate substituents attached to O-2 of Xyl^c and Xyl^b, respectively.

nonreducing terminus of the oligoglycosyl alditol is an L, S, or F (i.e., the last β-D-Glc*p* residue in the chain bears a β-D-Gal*p*-(1→2)-α-D-Xyl*p*, α-L-Ara*f*-(1→2)-α-D-Xyl*p* or α-L-Fuc*p*-(1→2)-β-D-Gal*p*-(1→2)-α-D-Xyl*p* side chain, respectively, at O-6), H-4 of the β-D-Glc*p* residue is shifted upfield (δ 3.46) relative to its position when the oligoglycosyl alditol is terminated by an X (δ 3.51–3.52). This places H-4 in a part of spectrum where few other resonances are found. Thus, the presence of a multiplet (dd, $^3J_{3,4} \sim 10$ and $^3J_{4,5} \sim 10$ Hz) with a chemical shift of 3.46 is diagnostic for the presence of a di- or triglycosyl side chain at O-6 of the β-D-Glc*p* residue at the nonreducing end of the oligoglycosyl alditol.

It should be mentioned that the presence of residual borate in the oligoglycosyl alditol samples can lead to misleading NMR data, as previously described.[22] The alditol readily forms borate esters when the pH is greater than 8, which affects the chemical shifts and intensities of several resonances in the ^{1}H NMR spectrum. Even though the large oligoglycosyl alditols XGGXXGGol, XXGGXGGol and XGGXSGGol had been through several purification steps, they still appeared to contain residual borate, leading to the broadening and shifting of some resonances and a decrease in their integrated area of other resonances. This was most obvious for the H-1 resonance of the β-D-Glc*p* residue directly attached to the alditol of these oligoglycosyl alditols, whose integrated area was approximately half the expected value. However, the ^{1}H NMR spectra of these molecules had narrow lines and appropriate integrated areas after the solution was acidified with CO_2 (pH < 7) to inhibit the formation of borate esters.

Long-range crosspeaks in the NOESY spectrum of LTGGol (Fig. 1) provide hints regarding the solution conformation of this oligoglycosyl alditol. For example, an unexpected crosspeak correlating α-Ara^b H-5 and Glc^a H-1 is present in the NOESY spectrum, even though these two nuclei are separated by 18 molecular bonds. The presence of this crosspeak suggests that LTGGol can (at least transiently) adopt a conformation in which the β-L-Ara*f*-(1→3)-α-L-Ara*f*-(1→2)-α-D-Xyl*p* (T) side chain points toward the alditol end. This is consistent with molecular models that indicate it is possible for α-Ara^b H-5 to come close to Glc^a H-1

when the side chain-bearing hydroxymethyl group of Glc[b] is in the *gt* conformation. More rigorous analyses of the relationships between the structure of xyloglucan and its conformations in solution are now being performed in our laboratory in order to learn more about the process of plant cell wall assembly and the structural requirements for this process.

Table 5
Ions in the MALDITOF MS of three large oligoglycosyl alditols from tomato xyloglucan and their XEG-generated fragments

Untreated	XEG-treated	XEG-treated then per-*O*-acetylated
1574 [a] (XGGXXGGol)	659 (XGG) 956 (XXGGol)	1206 [b] (XGG-Ac_{13}) 1753 [b] (XXGGol-Ac_{19})
1574 (XXGGXGGol)	660 (XGGol) 791 (XXG) 823 (GXGGol) 954 (XXGG)	1251 [b] (XGGol-Ac_{14}) 1423 [b] (XXG-Ac_{15}) 1539 [b] (GXGGol-Ac_{17}) 1711 [b] (XXGG-Ac_{18})
1706 (XGGXSGGol)	659 (XGG) 1088 (XSGGol)	not analyzed

[a] Data are m/z (± 3 Da) measured for $[M+Na]^+$ ions with the structural assignment in parenthesis.

[b] The spectra of the per-*O*-acetylated fragments also included less abundant $[M+K]^+$ ions along with ions indicating the presence of underacetylated products.

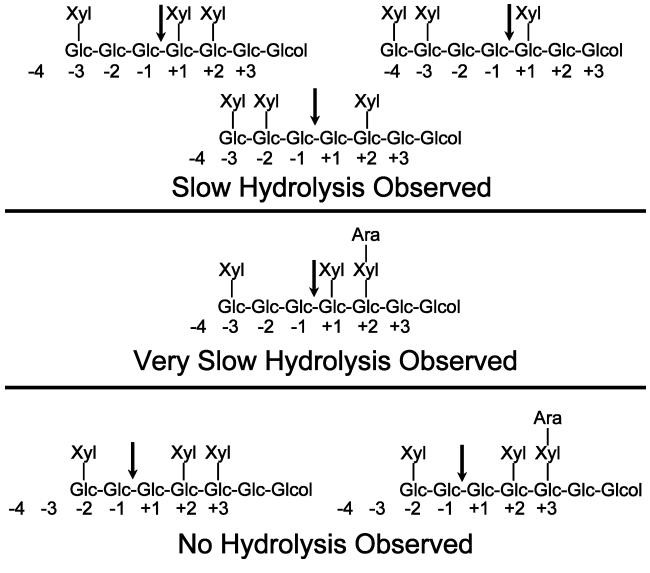

Fig. 3. Hydrolysis of tomato oligoglycosyl aditols by XEG. Sites of glycosidic bond cleavage are indicated by arrows. Efficient hydrolysis requires an unbranched β-(1→4)-linked glucosyl residue at the −1 site and a side chain-bearing glucosyl residue at the −3 site.

It is worthy of note that two different glycosidic bonds in XXGGXGGol appear to be susceptible to hydrolysis by XEG, leading to the formation of (XXGG + XGGol) and (XXG + GXGGol). The native xyloglucan contains *O*-acetyl substituents at O-6 of Glc[a] of each subunit,[12,14] making the glycosidic linkage of this residue resistant to hydrolysis by XEG and directing enzymatic attack to glycosidic bonds linking unbranched glucosyl residues to glucosyl residues that bear a side chain at O-6. Thus, the major products generated during XEG-treatment of the native polysaccharide are XXGG-type oligosaccharides. The hydrolysis of both unbranched Glc residues in XXGGXGGol is not entirely unexpected, as removal of the *O*-acetyl substituents during the reduction reaction makes both of the internal, unbranched β-D-Glc*p* residues susceptible to attack by XEG. However, XEG-treatment of XGGXXGGol led to the formation of XGG and XXGGol by cleaving the substrate almost exclusively between 'G' and 'X' with very little cleavage between the two 'G's. Furthermore, the arabinose-containing oligoglycosyl alditol XGGXSGGol appears to be especially resistant to XEG-catalyzed hydrolysis, and was hydrolyzed very slowly. Together, these results suggest that productive binding of oligoxyloglucan substrates to XEG depends on specific spatial relationships between xylosyl residues in the side chains (Fig. 3). That is, productive binding of the substrate appears to require an unbranched β-D-Glc*p* residue at the −1 binding subsite and a side chain-bearing β-D-Glc*p* residue at the −3 subsite. (See Davies and coworkers, for a description of the subsite nomenclature.[26]) The survival of XGGXXGG, XXGGXGG, and XGGXSGG in the original XEG-digestion suggests that they are cleaved slowly. This may be explained by hypothesizing that the simultaneous presence of side chain-bearing β-D-Glc*p* residues in the −4 and +2 subsites significantly increases the chances of productive binding. (XGGXXGG and XGGXSGG cannot occupy the −4 subsite when an unbranched β-D-Glc*p* residue is in the −1 subsite. Depending on the point of cleavage, XXGGXGG either does not occupy the −4 subsite or the β-D-Glc*p* residue in the +2 subsite is not branched.) The resistance of XGGXSGG to XEG-catalyzed hydrolysis suggests that an α-L-Ara*f*-(1→2)-α-D-Xyl*p* side chain at the +2 site decreases the chances of productive binding relative to the presence of a (monoglycosyl)-α-D-Xyl*p* side chain at this position. Additional experiments are necessary to completely characterize the substrate specificity of XEG.

4. Experimental

4.1. Preparation of xyloglucan

Tomato (*L. esculentum* 'Bonnie Best') cells[27] were cultured in the medium of Linsmaier and Skoog supplemented with 2,4-dichlorophenoxyacetic acid (2,4-D, 1 mg/mL).[28] Seven days after inoculation, cells were removed from the 20-L culture by filtration through a fine nylon net. The culture filtrate was precipitated by adding 4 vols of 95% EtOH and the precipitated polysaccharides were collected by centrifugation (20 min at 6000*g*). Acidic polysaccharides were removed by adjusting the pH of the solution to 7.0 with imidazole (final concentration 10 mM) and passing it through a column (100 mL) of Q-Sepharose (Pharmacia), eluted with the same buffer. The column eluant, containing the xyloglucan, was dialyzed versus deionized water and lyophilized (yield 6.6 g).

4.2. Endoglucanase treatment of xyloglucan

Tomato xyloglucan (6.6 g) was dissolved in 20 mM NaOAc buffer, pH 5, and it was passed through a Bio-Rad S Cartridge to remove proteins that had not been removed by Q-Sepharose. The eluant was treated with 100 U of XEG, generously provided by Novozymes (Copenhagen, Denmark) and purified as described.[15] The sample was incubated at room temperature (rt) for 48 h and monitored by MALDITOF MS. After hydrolysis was completed, 3 vols of 95% EtOH were added, and the resulting precipitate (mainly galactoglucomannan) was removed by centrifugation (10 min at 3000*g*). The supernatant containing the oligosaccharides was concentrated to remove EtOH and desalted on Sephadex G-25. Xyloglucan oligosaccharides were detected in the G-25 eluant by the anthrone assay for hexoses.[29] The salt-free fractions were pooled and lyophilized (700 mg).

4.3. Reduction of the oligosaccharides

The xyloglucan oligosaccharides were converted to the corresponding oligoglycosyl alditiol derivatives by reduction with $NaBH_4$ (10 mg/mL in 1 M NH_4OH, 20 mL). After incubating the reaction for 1 h at rt, the solution was chilled (0 °C), and the remaining borohydride was converted to borate by dropwise addition of acetone (1 mL). The solvent was evaporated and the residue was desalted on Sephadex G-25 as described above.

4.4. Gel-permeation chromatography

The desalted xyloglucan oligoglycosyl alditols were chromatographed on two Bio-Gel P-2 columns (-400 mesh, 96×1.6 cm) connected in series and eluted with deionized water.[20] Fractions (2.5 mL) were collected and assayed for carbohydrate content by the anthrone assay.

4.5. Liquid chromatography of oligoglycosyl alditols

Oligoglycosyl alditols were separated by reversed-phase HPLC on an octadecyl silica column (Hibar Lichrosob RP-18, 1.0×25 cm). Typically, individual Bio-Gel P-2 fractions were concentrated, and 100–200 μL of the resulting solution was injected onto the column and eluted with a gradient of aq MeOH (6–15% v/v at 2.0 mL/min). Oligoglycosyl alditols were detected by an evaporative light scattering detector (SEDEX 55 ELSD, S.E.D.E.R.E., Alfortville, France).

4.6. Matrix-assisted laser-induced/ionization time-of-flight mass spectrometry (MALDITOF MS)

MALDITOF mass spectra were recorded using a Hewlett–Packard LDI 1700 XP spectrometer operated at an accelerating voltage of 30 kV, an extractor voltage of 9 kV, and a source pressure of approx 8×10^{-7} torr. The matrix for oligosaccharides analysis was prepared by mixing (1:1 v/v) 2,5-dihydroxbenzoic acid (DHB, 0.2 M) and 1-hydroxyisoquinoline (HIC, 0.06 M), both in 50% aq MeCN.

4.7. Nuclear magnetic resonance (NMR) spectroscopy

Purified oligoglycosyl alditols were dissolved in 99.96% enriched ^2H_2O (600 μL) and transferred to a 5-mm NMR tube. Two-dimensional NMR spectra,[30] including gCOSY,[19] TOCSY, NOESY, gHSQC, and HMBC, were recorded at 298 K with a Varian Inova 600 NMR spectrometer using standard Varian pulse sequences. The TOCSY and NOESY mixing times were 100 and 500 ms, respectively. Pulsed field gradients were used for coherence selection in the gCOSY and gHSQC experiments. In a typical two-dimensional ($^1H-^1H$) spectrum, 512 FIDs consisting of 1024 data points were recorded with a spectral width of 1500 Hz in both dimensions, and the data were processed with zero filling to obtain 2048×2048 matrix. (For high resolution gCOSY spectra, 800 FIDs were recorded.) Chemical shifts were measured relative to internal acetone at δ 2.225.

Acknowledgements

The authors thank Novozymes A/S for generously providing the xyloglucan-specific endoglucanase (XEG). This research is supported in part by funds from the U.S. Department of Energy, grants DE-FG05-93ER20097 and DE-FG02-96ER20220.

References

1. McCann, M. C.; Roberts, K. In *The Cytoskeletal Basis of Plant Growth and Form*; Lloyd, C. W., Ed.; Academic Press: London, 1991; pp 109–129.
2. Talbot, L. F.; Ray, P. M. *Plant Physiol.* **1992**, *98*, 357–368.
3. Carpita, N. C.; Gibeaut, D. M. *Plant J.* **1993**, *3*, 1–30.
4. McCann, M. C.; Roberts, K. *J. Exp. Bot.* **1994**, *45*, 1683–1691.
5. Ha, M. A.; Apperly, D. C.; Jarvis, M. *Plant Physiol.* **1997**, *115*, 593–598.
6. Levy, S.; Maclachlan, G.; Staehelin, L. A. *Plant J.* **1997**, *11*, 373–386.
7. York, W. S.; Darvill, A. G.; Albersheim, P. *Plant Physiol.* **1984**, *75*, 295–297.
8. Vanzin, G. F.; Madison, M.; Carpita, N. C.; Raikhel, N. V.; Keegstra, K.; Reiter, W.-D. *Proc. Natl. Acad. Sci. USA* **2002**, *99*, 3340–3345.
9. Perrin R.M.; Jia Z.; Wagner T.A.; O'Neill M.A.; Sarria R.; York W.S.; Raikhel N.V.; Keegstra K. *Plant Physiol.* **2002**, submitted.
10. Fry, S. C.; York, W. S.; Albersheim, P.; Darvill, A. G.; Hayashi, T.; Joseleau, J. P.; Kato, Y.; Lorences, E. P.; Maclachlan, G. A.; McNeil, M.; Mort, A. J.; Reid, J. S. G.; Seitz, H.-U.; Selvendran, R. R.; Shibaev, V. N.; Voragen, A. G. J.; White, A. R. *Physiol. Plantarum* **1993**, *89*, 1–3.
11. Vincken, J.-P.; York, W. S.; Beldman, G.; Voragen, A. G. J. *Plant Physiol.* **1997**, *114*, 9–12.
12. York, W. S.; Kolli, V. S. K.; Orlando, R.; Albersheim, P.; Darvill, A. G. *Carbohydr. Res.* **1996**, *285*, 99–128.
13. Vierhuis, E.; York, W. S.; Vincken, J.-P.; Schols, H. A.; Van Alebeek, G.-J. W. M.; Voragen, A. G. J. *Carbohydr. Res.* **2001**, *332*, 285–397.
14. Sims, I. M.; Craik, D. J.; Bacic, A. *Carbohydr. Res.* **1997**, *303*, 79–92.
15. Pauly, M.; Andersen, L. N.; Kaupinen, S.; Kofod, L. V.; York, W. S.; Albersheim, P.; Darvill, A. G. *Glycobiology* **1999**, *9*, 93–100.
16. Vincken J.-P.; Beldman, G.; Voragen, A.G.J. *Carbohydr. Res.* **1997**, *298*, 299–310.
17. Homans, S. W. *Prog. NMR Spectrosc.* **1990**, *22*, 55–81.
18. Neuhaus, D.; Williamson, M. P. *The Nuclear Overhauser Effect in Structural Calculations*; VCH Publishers: New York, 1989.
19. Otter, A.; Bundle, D. R. *J. Magn. Reson. (B)* **1995**, *109*, 194–201.
20. York, W. S.; Van Halbeek, H.; Darvill, A. G.; Albersheim, P. *Carbohydr. Res.* **1990**, *200*, 9–31.
21. Hisamatsu, M.; York, W. S.; Darvill, A. G.; Albersheim, P. *Carbohydr. Res.* **1992**, *227*, 45–71.
22. York, W. S.; Harvey, L. K.; Guillen, R.; Albersheim, P.; Darvill, A. G. *Carbohydr. Res.* **1993**, *248*, 285–301.
23. York, W. S.; Impallomeni, G.; Hisamatsu, M.; Albersheim, P.; Darvill, A. *Carbohydr. Res.* **1994**, *267*, 79–104.
24. Hantus, S.; Pauly, M.; Darvill, A. G.; Albersheim, P.; York, W. S. *Carbohydr. Res.* **1997**, *304*, 11–20.
25. Vliegenthart, J. F. G.; Dorland, L.; Van Halbeek, H. *Adv. Carbohydr. Chem. Biochem.* **1983**, *41*, 209–374.
26. Davies, G. J.; Wilson, K. S.; Henrissat, B. *Biochem. J.* **1997**, *321*, 557–559.
27. Smith, J. J.; Muldoon, E. P.; Lamport, D. T. A. *Phytochemistry* **1984**, *23*, 1233–1239.
28. DuPont, F. M.; Staraci, L. C.; Chou, B.; Thomas, B. R.; Williams, B. G.; Mudd, J. B. *Plant Physiol.* **1985**, *77*, 64–68.
29. Dische, Z. *Methods Carbohydr. Chem.* **1962**, *1*, 478–481.
30. Kessler, H.; Gehrke, M.; Griesinger, C. *Angew. Chem., Int. Ed. Engl.* **1988**, *27*, 447–592.